EUROPEAN ORGANIZATION FOR NUCLEAR RESEARCH

CERN–EP/98–75

13 May 1998

Measurement of the $e^+e^- \to \gamma\gamma(\gamma)$ cross section at the LEP energies

DELPHI Collaboration

Abstract

The total and the differential cross-sections for the reaction $e^+e^- \to \gamma\gamma(\gamma)$ have been measured with the DELPHI detector at LEP at centre-of-mass energies from 130 to 183 GeV for an integrated luminosity of 78.19. pb^{-1}. The results agree with the QED predictions. The lower limits (obtained including previously published results at the Z^0 energies) on the QED cutoff parameters are $\Lambda_+ > 253$ GeV and $\Lambda_- > 225$ GeV and the lower bound on the mass of an excited electron with an effective coupling constant $\lambda_\gamma = 1$ is 231 GeV/c^2. All the limits are at the 95% confidence level.

(Submitted to Phys. Lett. B)

P.Abreu[21], W.Adam[49], T.Adye[36], P.Adzic[11], G.D.Alekseev[16], R.Alemany[48], P.P.Allport[22], S.Almehed[24], U.Amaldi[9], S.Amato[46], P.Andersson[43], A.Andreazza[9], P.Antilogus[25], W-D.Apel[17], Y.Arnoud[14], B.Åsman[43], J-E.Augustin[25], A.Augustinus[9], P.Baillon[9], P.Bambade[19], F.Barao[21], R.Barbier[25], D.Y.Bardin[16], G.Barker[9], A.Baroncelli[39], O.Barring[24], M.Battaglia[15], M.Baubillier[23], K-H.Becks[51], M.Begalli[6], P.Beilliere[8], Yu.Belokopytov[9,52], K.Belous[41], A.C.Benvenuti[5], C.Berat[14], M.Berggren[25], D.Bertini[25], D.Bertrand[2], M.Besancon[38], F.Bianchi[44], M.Bigi[44], M.S.Bilenky[16], M-A.Bizouard[19], D.Bloch[10], M.Bonesini[27], W.Bonivento[27], M.Boonekamp[38], P.S.L.Booth[22], A.W.Borgland[4], G.Borisov[38], C.Bosio[39], O.Botner[47], E.Boudinov[30], B.Bouquet[19], C.Bourdarios[19], T.J.V.Bowcock[22], I.Boyko[16], I.Bozovic[11], M.Bozzo[13], P.Branchini[39], T.Brenke[51], R.A.Brenner[47], P.Bruckman[35], J-M.Brunet[8], L.Bugge[32], T.Buran[32], T.Burgsmueller[51], P.Buschmann[51], S.Cabrera[48], M.Caccia[27], M.Calvi[27], A.J.Camacho Rozas[40], T.Camporesi[9], V.Canale[37], M.Canepa[13], F.Carena[9], L.Carroll[22], C.Caso[13], M.V.Castillo Gimenez[48], A.Cattai[9], F.R.Cavallo[5], Ch.Cerruti[10], V.Chabaud[9], M.Chapkin[41], Ph.Charpentier[9], L.Chaussard[25], P.Checchia[35], G.A.Chelkov[16], M.Chen[2], R.Chierici[44], P.Chliapnikov[41], P.Chochula[7], V.Chorowicz[25], J.Chudoba[29], P.Collins[9], M.Colomer[48], R.Contri[13], E.Cortina[48], G.Cosme[19], F.Cossutti[38], J-H.Cowell[22], H.B.Crawley[1], D.Crennell[36], G.Crosetti[13], J.Cuevas Maestro[33], S.Czellar[15], B.Dalmagne[19], G.Damgaard[28], M.Davenport[9], W.Da Silva[23], A.Deghorain[2], G.Della Ricca[45], P.Delpierre[26], N.Demaria[9], A.De Angelis[9], W.De Boer[17], S.De Brabandere[2], C.De Clercq[2], B.De Lotto[45], A.De Min[35], L.De Paula[46], H.Dijkstra[9], L.Di Ciaccio[37], A.Di Diodato[37], A.Djannati[8], J.Dolbeau[8], K.Doroba[50], M.Dracos[10], J.Drees[51], K.-A.Drees[51], M.Dris[31], A.Duperrin[25], J-D.Durand[25,9], R.Ehret[17], G.Eigen[4], T.Ekelof[47], G.Ekspong[43], M.Ellert[47], M.Elsing[9], J-P.Engel[10], B.Erzen[42], M.Espirito Santo[21], E.Falk[24], G.Fanourakis[11], D.Fassouliotis[11], J.Fayot[23], M.Feindt[17], A.Fenyuk[41], P.Ferrari[27], A.Ferrer[48], S.Fichet[23], A.Firestone[1], P.-A.Fischer[9], U.Flagmeyer[51], H.Foeth[9], E.Fokitis[31], F.Fontanelli[13], B.Franek[36], A.G.Frodesen[4], R.Fruhwirth[49], F.Fulda-Quenzer[19], J.Fuster[48], A.Galloni[22], D.Gamba[44], M.Gandelman[46], C.Garcia[48], J.Garcia[40], C.Gaspar[9], M.Gaspar[46], U.Gasparini[35], Ph.Gavillet[9], E.N.Gazis[31], D.Gele[10], J-P.Gerber[10], N.Ghodbane[25], I.Gil[48], F.Glege[51], R.Gokieli[50], B.Golob[42], P.Goncalves[21], I.Gonzalez Caballero[40], G.Gopal[36], L.Gorn[1,53], M.Gorski[50], Yu.Gouz[41], V.Gracco[13], J.Grahl[1], E.Graziani[39], C.Green[22], A.Grefrath[51], P.Gris[38], G.Grosdidier[19], K.Grzelak[50], M.Gunther[47], J.Guy[36], F.Hahn[9], S.Hahn[51], S.Haider[9], A.Hallgren[47], K.Hamacher[51], F.J.Harris[34], V.Hedberg[24], S.Heising[17], R.Henriques[21], J.J.Hernandez[48], P.Herquet[2], H.Herr[9], T.L.Hessing[34], J.-M.Heuser[51], E.Higon[48], S-O.Holmgren[43], P.J.Holt[34], D.Holthuizen[30], S.Hoorelbeke[2], M.Houlden[22], J.Hrubec[49], K.Huet[2], K.Hultqvist[43], J.N.Jackson[22], R.Jacobsson[43], P.Jalocha[9], R.Janik[7], Ch.Jarlskog[24], G.Jarlskog[24], P.Jarry[38], B.Jean-Marie[19], E.K.Johansson[43], L.Jonsson[24], P.Jonsson[24], C.Joram[9], P.Juillot[10], F.Kapusta[23], K.Karafasoulis[11], S.Katsanevas[25], E.C.Katsoufis[31], R.Keranen[17], B.A.Khomenko[16], N.N.Khovanski[16], B.King[22], N.J.Kjaer[30], O.Klapp[51], H.Klein[9], P.Kluit[30], D.Knoblauch[17], P.Kokkinias[11], A.Konopliannikov[41], M.Koratzinos[9], V.Kostioukhine[41], C.Kourkoumelis[3], O.Kouznetsov[16], M.Krammer[49], C.Kreuter[9], I.Kronkvist[24], J.Krstic[11], Z.Krumstein[16], P.Kubinec[7], W.Kucewicz[18], K.Kurvinen[15], J.W.Lamsa[1], L.Lanceri[45], D.W.Lane[1], P.Langefeld[51], V.Lapin[41], J-P.Laugier[38], R.Lauhakangas[15], G.Leder[49], F.Ledroit[14], V.Lefebure[2], L.Leinonen[43], A.Leisos[11], R.Leitner[29], J.Lemonne[2], G.Lenzen[51], V.Lepeltier[19], T.Lesiak[18], M.Lethuillier[38], J.Libby[34], D.Liko[9], A.Lipniacka[43], I.Lippi[35], B.Loerstad[24], J.G.Loken[34], J.H.Lopes[46], J.M.Lopez[40], R.Lopez-Fernandez[14], D.Loukas[11], P.Lutz[38], L.Lyons[34], J.MacNaughton[49], J.R.Mahon[6], A.Maio[21], A.Malek[51], T.G.M.Malmgren[43], V.Malychev[16], F.Mandl[49], J.Marco[40], R.Marco[40], B.Marechal[46], M.Margoni[35], J-C.Marin[9], C.Mariotti[9], A.Markou[11], C.Martinez-Rivero[33], F.Martinez-Vidal[48], S.Marti i Garcia[22], F.Matorras[40], C.Matteuzzi[27], G.Matthiae[37], F.Mazzucato[35], M.Mazzucato[35], M.Mc Cubbin[22], R.Mc Kay[1], R.Mc Nulty[9], G.Mc Pherson[22], C.Meroni[27], E.Migliore[44], L.Mirabito[25], W.A.Mitaroff[49], U.Mjoernmark[24], T.Moa[43], R.Moeller[28], K.Moenig[9], M.R.Monge[13], X.Moreau[23], P.Morettini[13], G.Morton[34], K.Muenich[51], M.Mulders[30], C.Mulet-Marquis[14], W.J.Murray[36], B.Muryn[14,18], G.Myatt[34], T.Myklebust[32], F.Naraghi[14], F.L.Navarria[5], S.Navas[48], K.Nawrocki[50], P.Negri[27], S.Nemecek[12], N.Neufeld[9], W.Neumann[51], N.Neumeister[49], R.Nicolaidou[14], B.S.Nielsen[28], M.Nieuwenhuizen[30], V.Nikolaenko[10], M.Nikolenko[10,16], A.Normand[22], A.Nygren[24], V.Obraztsov[41], A.G.Olshevski[16], A.Onofre[21], R.Orava[15], G.Orazi[10], K.Osterberg[15], A.Ouraou[38], P.Paganini[19], M.Paganoni[27], S.Paiano[5], R.Pain[23], R.Paiva[21], J.Palacios[34], H.Palka[18], Th.D.Papadopoulou[31], K.Papageorgiou[11], L.Pape[9], C.Parkes[34], F.Parodi[13], U.Parzefall[22], A.Passeri[39], M.Pegoraro[35], L.Peralta[21], A.Perrotta[5], C.Petridou[45], A.Petrolini[13], H.T.Phillips[36], G.Piana[13], F.Pierre[38], M.Pimenta[21], E.Piotto[27], T.Podobnik[42], M.E.Pol[6], G.Polok[18], P.Poropat[45], V.Pozdniakov[16], P.Privitera[37], N.Pukhaeva[16], A.Pullia[27], D.Radojicic[34], S.Ragazzi[27], H.Rahmani[31], D.Rakoczy[49], J.Rames[12], P.N.Ratoff[20], A.L.Read[32], P.Rebecchi[9], N.G.Redaelli[27], M.Regler[49], D.Reid[9], R.Reinhardt[51], P.B.Renton[34], L.K.Resvanis[3], F.Richard[19], J.Ridky[12], G.Rinaudo[44], O.Rohne[32], A.Romero[44], P.Ronchese[35], E.I.Rosenberg[1], P.Rosinsky[7], P.Roudeau[19], T.Rovelli[5], V.Ruhlmann-Kleider[38], A.Ruiz[40], H.Saarikko[15], Y.Sacquin[38], A.Sadovsky[16], G.Sajot[14], J.Salt[48], D.Sampsonidis[11], M.Sannino[13], H.Schneider[17], Ph.Schwemling[23], U.Schwickerath[17], M.A.E.Schyns[51], F.Scuri[45], P.Seager[20], Y.Sedykh[16], A.M.Segar[34], R.Sekulin[36], R.C.Shellard[6], A.Sheridan[22], R.Silvestre[38], L.Simard[38], F.Simonetto[35], A.N.Sisakian[16], T.B.Skaali[32], G.Smadja[25], O.Smirnova[24], G.R.Smith[36], A.Sopczak[17], R.Sosnowski[50], T.Spassov[21], E.Spiriti[39], P.Sponholz[51], S.Squarcia[13], D.Stampfer[49], C.Stanescu[39], S.Stanic[42], S.Stapnes[32], K.Stevenson[34], A.Stocchi[19], J.Strauss[49], R.Strub[10], B.Stugu[4], M.Szczekowski[50], M.Szeptycka[50], T.Tabarelli[27], F.Tegenfeldt[47], F.Terranova[27], J.Thomas[34], A.Tilquin[26], J.Timmermans[30], L.G.Tkatchev[16], T.Todorov[10], S.Todorova[10], D.Z.Toet[30], A.Tomaradze[2], B.Tome[21], A.Tonazzo[27], L.Tortora[39], G.Transtromer[24],

D.Treille[9], G.Tristram[8], A.Trombini[19], C.Troncon[27], A.Tsirou[9], M-L.Turluer[38], I.A.Tyapkin[16], S.Tzamarias[11], B.Ueberschaer[51], O.Ullaland[9], V.Uvarov[41], G.Valenti[5], E.Vallazza[45], G.W.Van Apeldoorn[30], P.Van Dam[30], J.Van Eldik[30], A.Van Lysebetten[2], I.Van Vulpen[30], N.Vassilopoulos[34], G.Vegni[27], L.Ventura[35], W.Venus[36], F.Verbeure[2], M.Verlato[35], L.S.Vertogradov[16], V.Verzi[37], D.Vilanova[38], L.Vitale[45], E.Vlasov[41], A.S.Vodopyanov[16], V.Vrba[12], H.Wahlen[51], C.Walck[43], C.Weiser[17], A.M.Wetherell[9], D.Wicke[51], J.H.Wickens[2], G.R.Wilkinson[9], M.Winter[10], M.Witek[18], T.Wlodek[19], G.Wolf[9], J.Yi[1], O.Yushchenko[41], A.Zaitsev[41], A.Zalewska[18], P.Zalewski[50], D.Zavrtanik[42], E.Zevgolatakos[11], N.I.Zimin[16], G.C.Zucchelli[43], G.Zumerle[35]

[1] Department of Physics and Astronomy, Iowa State University, Ames IA 50011-3160, USA
[2] Physics Department, Univ. Instelling Antwerpen, Universiteitsplein 1, BE-2610 Wilrijk, Belgium
and IIHE, ULB-VUB, Pleinlaan 2, BE-1050 Brussels, Belgium
and Faculté des Sciences, Univ. de l'Etat Mons, Av. Maistriau 19, BE-7000 Mons, Belgium
[3] Physics Laboratory, University of Athens, Solonos Str. 104, GR-10680 Athens, Greece
[4] Department of Physics, University of Bergen, Allégaten 55, NO-5007 Bergen, Norway
[5] Dipartimento di Fisica, Università di Bologna and INFN, Via Irnerio 46, IT-40126 Bologna, Italy
[6] Centro Brasileiro de Pesquisas Físicas, rua Xavier Sigaud 150, BR-22290 Rio de Janeiro, Brazil
and Depto. de Física, Pont. Univ. Católica, C.P. 38071 BR-22453 Rio de Janeiro, Brazil
and Inst. de Física, Univ. Estadual do Rio de Janeiro, rua São Francisco Xavier 524, Rio de Janeiro, Brazil
[7] Comenius University, Faculty of Mathematics and Physics, Mlynska Dolina, SK-84215 Bratislava, Slovakia
[8] Collège de France, Lab. de Physique Corpusculaire, IN2P3-CNRS, FR-75231 Paris Cedex 05, France
[9] CERN, CH-1211 Geneva 23, Switzerland
[10] Institut de Recherches Subatomiques, IN2P3 - CNRS/ULP - BP20, FR-67037 Strasbourg Cedex, France
[11] Institute of Nuclear Physics, N.C.S.R. Demokritos, P.O. Box 60228, GR-15310 Athens, Greece
[12] FZU, Inst. of Phys. of the C.A.S. High Energy Physics Division, Na Slovance 2, CZ-180 40, Praha 8, Czech Republic
[13] Dipartimento di Fisica, Università di Genova and INFN, Via Dodecaneso 33, IT-16146 Genova, Italy
[14] Institut des Sciences Nucléaires, IN2P3-CNRS, Université de Grenoble 1, FR-38026 Grenoble Cedex, France
[15] Helsinki Institute of Physics, HIP, P.O. Box 9, FI-00014 Helsinki, Finland
[16] Joint Institute for Nuclear Research, Dubna, Head Post Office, P.O. Box 79, RU-101 000 Moscow, Russian Federation
[17] Institut für Experimentelle Kernphysik, Universität Karlsruhe, Postfach 6980, DE-76128 Karlsruhe, Germany
[18] Institute of Nuclear Physics and University of Mining and Metalurgy, Ul. Kawiory 26a, PL-30055 Krakow, Poland
[19] Université de Paris-Sud, Lab. de l'Accélérateur Linéaire, IN2P3-CNRS, Bât. 200, FR-91405 Orsay Cedex, France
[20] School of Physics and Chemistry, University of Lancaster, Lancaster LA1 4YB, UK
[21] LIP, IST, FCUL - Av. Elias Garcia, 14-1°, PT-1000 Lisboa Codex, Portugal
[22] Department of Physics, University of Liverpool, P.O. Box 147, Liverpool L69 3BX, UK
[23] LPNHE, IN2P3-CNRS, Univ. Paris VI et VII, Tour 33 (RdC), 4 place Jussieu, FR-75252 Paris Cedex 05, France
[24] Department of Physics, University of Lund, Sölvegatan 14, SE-223 63 Lund, Sweden
[25] Université Claude Bernard de Lyon, IPNL, IN2P3-CNRS, FR-69622 Villeurbanne Cedex, France
[26] Univ. d'Aix - Marseille II - CPP, IN2P3-CNRS, FR-13288 Marseille Cedex 09, France
[27] Dipartimento di Fisica, Università di Milano and INFN, Via Celoria 16, IT-20133 Milan, Italy
[28] Niels Bohr Institute, Blegdamsvej 17, DK-2100 Copenhagen Ø, Denmark
[29] NC, Nuclear Centre of MFF, Charles University, Areal MFF, V Holesovickach 2, CZ-180 00, Praha 8, Czech Republic
[30] NIKHEF, Postbus 41882, NL-1009 DB Amsterdam, The Netherlands
[31] National Technical University, Physics Department, Zografou Campus, GR-15773 Athens, Greece
[32] Physics Department, University of Oslo, Blindern, NO-1000 Oslo 3, Norway
[33] Dpto. Fisica, Univ. Oviedo, Avda. Calvo Sotelo s/n, ES-33007 Oviedo, Spain
[34] Department of Physics, University of Oxford, Keble Road, Oxford OX1 3RH, UK
[35] Dipartimento di Fisica, Università di Padova and INFN, Via Marzolo 8, IT-35131 Padua, Italy
[36] Rutherford Appleton Laboratory, Chilton, Didcot OX11 OQX, UK
[37] Dipartimento di Fisica, Università di Roma II and INFN, Tor Vergata, IT-00173 Rome, Italy
[38] DAPNIA/Service de Physique des Particules, CEA-Saclay, FR-91191 Gif-sur-Yvette Cedex, France
[39] Istituto Superiore di Sanità, Ist. Naz. di Fisica Nucl. (INFN), Viale Regina Elena 299, IT-00161 Rome, Italy
[40] Instituto de Fisica de Cantabria (CSIC-UC), Avda. los Castros s/n, ES-39006 Santander, Spain
[41] Inst. for High Energy Physics, Serpukov P.O. Box 35, Protvino, (Moscow Region), Russian Federation
[42] J. Stefan Institute, Jamova 39, SI-1000 Ljubljana, Slovenia and Department of Astroparticle Physics, School of Environmental Sciences, Kostanjeviska 16a, Nova Gorica, SI-5000 Slovenia,
and Department of Physics, University of Ljubljana, SI-1000 Ljubljana, Slovenia
[43] Fysikum, Stockholm University, Box 6730, SE-113 85 Stockholm, Sweden
[44] Dipartimento di Fisica Sperimentale, Università di Torino and INFN, Via P. Giuria 1, IT-10125 Turin, Italy
[45] Dipartimento di Fisica, Università di Trieste and INFN, Via A. Valerio 2, IT-34127 Trieste, Italy
and Istituto di Fisica, Università di Udine, IT-33100 Udine, Italy
[46] Univ. Federal do Rio de Janeiro, C.P. 68528 Cidade Univ., Ilha do Fundão BR-21945-970 Rio de Janeiro, Brazil
[47] Department of Radiation Sciences, University of Uppsala, P.O. Box 535, SE-751 21 Uppsala, Sweden
[48] IFIC, Valencia-CSIC, and D.F.A.M.N., U. de Valencia, Avda. Dr. Moliner 50, ES-46100 Burjassot (Valencia), Spain
[49] Institut für Hochenergiephysik, Österr. Akad. d. Wissensch., Nikolsdorfergasse 18, AT-1050 Vienna, Austria
[50] Inst. Nuclear Studies and University of Warsaw, Ul. Hoza 69, PL-00681 Warsaw, Poland
[51] Fachbereich Physik, University of Wuppertal, Postfach 100 127, DE-42097 Wuppertal, Germany
[52] On leave of absence from IHEP Serpukhov
[53] Now at University of Florida

1 Introduction

The reaction $e^+e^- \to \gamma\gamma(\gamma)$ provides a clean test of QED at LEP energies and is well suited to detect the presence of non-standard physics. Previous letters from the DELPHI collaboration [1,2] reported on a study of this reaction at the Z^0 energies based on 36.9 pb^{-1}. Similar results were published by other LEP collaborations [3]. In this letter a measurement of the $e^+e^- \to \gamma\gamma(\gamma)$ cross-section is reported using 78.2 pb^{-1} of data collected by DELPHI during the 1995, 1996 and 1997 runs at 130, 136, 161, 172 and 183 GeV centre-of-mass energies. These results are combined with the previously published results at the Z^0 pole [2] and are used to obtain limits on deviations from QED and to search for compositeness.

2 Apparatus

A detailed description of the DELPHI detector can be found in Ref.[4,5]. The present analysis was mainly based on the measurement of the electromagnetic energy clusters [6] in the barrel electromagnetic calorimeter, the High density Projection Chamber (HPC), and in the Forward ElectroMagnetic Calorimeter (FEMC) as well as on the capability of vetoing charged particles using the tracking devices. In addition to the track reconstruction in the Time Projection Chamber (TPC), Inner Detector (ID) and Outer Detector (OD), a very efficient way of rejecting final states which include charged particles was to use hits reconstructed in the Vertex Detector (VD).

The Vertex Detector [2] was upgraded in 1994 by introducing a double coordinate measurement in the layer closest to (6.5 cm) and furthest from (11 cm) the interaction point [7]. In 1996 the detector was extended to cover the polar angle (θ) region [1] between 25° and 155° and the double coordinate measurement was introduced in the central layer between 25° and 45° and between 135° and 155° [8]. Since 1994, a new electromagnetic calorimeter (STIC) was used to measure the luminosity.

The barrel and the forward electromagnetic energy trigger was based on data from the HPC and the FEMC, respectively. The HPC trigger consists of a 1st level trigger based on scintillator plates inserted into the calorimeter at the depth corresponding to the maximum development of electromagnetic showers. The barrel electromagnetic energy trigger then requires coincidence with a 2nd level trigger based on the energy release on the calorimeter modules. The FEMC trigger simply rely on energy deposition on the lead-glass counters. A detailed description of the DELPHI trigger can be found in [5]. Because of the increased LEP luminosity and the correspondingly higher backgrounds, the trigger contained less redundancy than that used for the analysis on the Z^0 pole. The efficiency was therefore poorer and had to be measured as a function of the different running periods. The trigger efficiency for $e^+e^- \to \gamma\gamma(\gamma)$ was measured by noting how often the electromagnetic energy trigger was fired by e^+e^- final state events which had been triggered by an independent track trigger.

The results obtained are shown in Table 1. The low value measured in the 172 GeV run was due to a hardware failure in the second period of the 1996 data-taking. Compatible results were obtained from multi-photon final state events by looking at the correspondence between the trigger signal multiplicity and the number of detected photons.

[1] The DELPHI coordinate system is Cartesian with the z axis along the electron direction, the x axis pointing towards the LEP centre and the y axis pointing upwards. The polar angle $\theta = tg^{-1}(\sqrt{x^2+y^2}/z)$ and the azimuthal angle $\phi = tg^{-1}(y/x)$.

$\sqrt{s}$ GeV	Barrel Efficiency	Forward Efficiency
1995 data		
133.4	$0.986^{+0.011}_{-0.022}$	-
1996 data		
161.5	0.956 ± 0.013	> 0.995
172.4	0.775 ± 0.025	> 0.995
1997 data		
182.7	0.990 ± 0.005	> 0.995

Table 1: Efficiency for the barrel and forward electromagnetic trigger as a function of the different running periods. The efficiency of two 1995 energy points is given at the mean centre-of-mass energy, weighted by the luminosity at each point.

3 Event selection and analysis

The data of 1995 were collected at two LEP centre-of-mass energies, 130.4 GeV and 136.3 GeV, the data of 1996 at 161.5 GeV and 172.4 GeV whereas the 1997 data-set was taken at the mean energy of 182.7 GeV. Requiring that the HPC, FEMC, TPC and VD were operational, the integrated luminosities at each energy point were 2.86 pb^{-1}, 2.96 pb^{-1} 9.58 pb^{-1}, 9.80 pb^{-1} and 52.99 pb^{-1}, respectively.

The analysis was similar to the one reported in [2]. Events with energetic clusters in the electromagnetic calorimeters were selected. Charged particle final states (mainly e^+e^- final state events) were rejected using a Vertex Detector track search which required that there were hits in at least two of the three VD layers, which were aligned with the mean beam crossing point. The use of the VD confined the analysis to the barrel region for the 1995 data, while the VD upgrade allowed the analysis to be extended into the forward region (corresponding to the FEMC acceptance) for data taken in 1996 and 1997. Although suppressing background, vetoing tracks using a VD track search also removed a small number of signal events where a photon converted into e^+e^- before or in the region of sensitivity of the Vertex Detector.

Charged particle final states were also rejected by looking for tracks (TK) in the other tracking devices. The redundancy of this search allowed the efficiency of the VD search to be measured, while also removing the small number of e^+e^- final state events with both VD tracks missing.

Events were selected as $\gamma\gamma(\gamma)$ candidates if they satisfied the following criteria :
- at least two electromagnetic energy clusters with $0.219 < E/\sqrt{s} < 0.713$ GeV;
- at least two electromagnetic energy clusters in the HPC, ($42° < \theta < 88°$ or $92° < \theta < 138°$) or in the FEMC ($25° < \theta < 32.4°$ or $147.6° < \theta < 155°$) ;
- acollinearity between the two most energetic clusters smaller than 30°;
- no tracks reconstructed in the Vertex Detector associated to the HPC or FEMC clusters ($\pm 2°$ in the azimuthal angle ϕ) ;
- two hemispheres were defined by the direction of the most energetic cluster. In the barrel region, one hemisphere was required to have no TK with a momentum greater than 1 GeV/c which extrapolated to within 5 cm of the mean beam crossing point. In the forward region, the requirement was strengthened to suppress the larger e^+e^- background further, by demanding that both hemispheres have no such TK.

The samples obtained after applying these requirements in the barrel (HPC) region are listed in Table 2 for the different years and LEP energies. Including the data reported in [2], a total of 803 $\gamma\gamma(\gamma)$ events were obtained from the barrel region and 89 from the forward region. The ability of these selection criteria to separate $\gamma\gamma(\gamma)$ events from the e^+e^- background can be seen in Fig.1 which shows the difference in azimuth $(180^\circ - \Delta\phi)$ between the two most energetic clusters[2] for both types of events at 183 GeV centre-of-mass energy. The $\gamma\gamma(\gamma)$ events do not exhibit the effect of the magnetic field bending as e^+e^- final state events do.

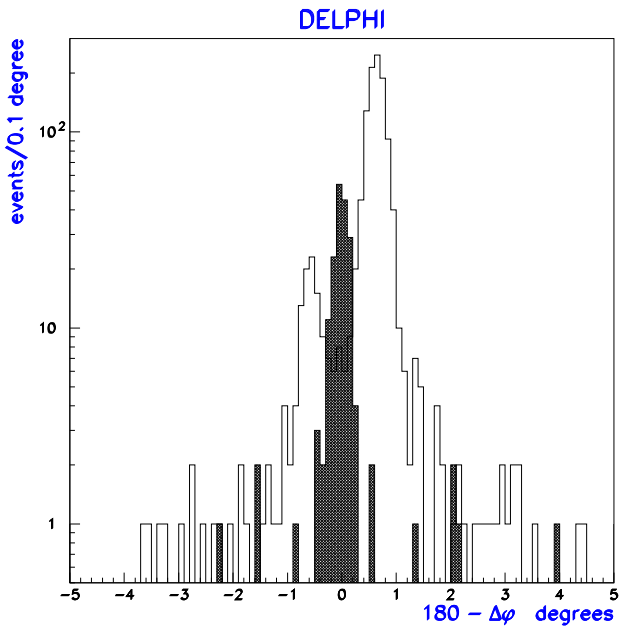

Figure 1: Distribution of the difference $180^\circ - \Delta\phi$ between the two most energetic clusters for e^+e^- (white area) and $\gamma\gamma(\gamma)$ events (hatched area) at 183 GeV centre-of-mass energy. The difference in height between the two e^+e^- peaks reflects the physical forward-backward asymmetry of such events.

The energy sum of the two most energetic clusters, for the data taken at 183 GeV, is shown in Fig.2. It is compared with the same quantity obtained with a simulated sample of $\gamma\gamma(\gamma)$ events [9] processed through the DELPHI detector simulation [5] and the same analysis chain as the real data.

The cosine of the scattering angle is defined as $\cos\theta = \left|\frac{\cos\frac{1}{2}(\theta_1+\pi-\theta_2)}{\cos\frac{1}{2}(\theta_1-\pi+\theta_2)}\right|$ where θ_1 and θ_2 are the polar angles of the two most energetic photons. This definition has the advantage of not being sensitive to the collinear initial state radiation. The efficiency obtained with the selection criteria defined above was determined in different $\cos\theta$ intervals with the $\gamma\gamma(\gamma)$ Monte Carlo sample. The global efficiency for accepting $\gamma\gamma(\gamma)$ events, integrated over the whole barrel acceptance region, was $(89.4 \pm 2.5)\%$, where the error includes the Monte Carlo statistics, the error on the acceptance definition and the stability of the result with respect to variations on the energy and acceptance cuts. In e^+e^- final state events the efficiency of the calorimeter and VD selection can be measured directly on

[2] The quantity $180^\circ - \Delta\phi$ is defined as $\phi_+ - \phi_- - 180 \cdot sign(\phi_+ - \phi_-)$ where ϕ_+ (ϕ_-) refers to the azimuth of the cluster with the larger (smaller) z coordinate.

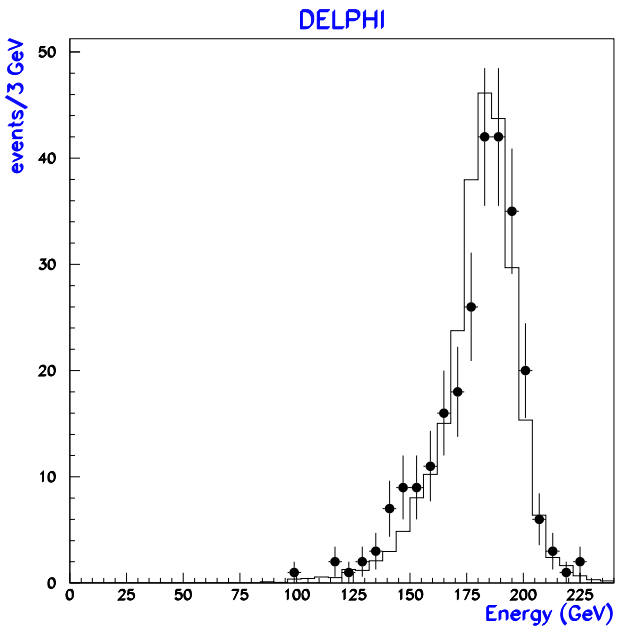

Figure 2: The energy sum of the two most energetic clusters for 183 GeV data (dots) and simulation (full line) events.

the data with an alternative selection based on TKs [5]. The efficiency was defined as the ratio between the number of the events selected with both the calorimetric and TK selection and the number of the events selected with the TK selection. This procedure can be repeated in simulated events and the efficiency obtained can be compared with the one obtained in the real data. The comparison allows the calorimeter and the VD response to be monitored since agreement is expected when both are working properly. For all the periods the agreement was good except for the 1997 run when the efficiency on the real data was lower by $(4.3 \pm 1.4)\%$. The difference was understood to be due to a loss caused by beam background tracks seen in VD and accidentally associated to the electromagnetic clusters. The correction was applied and its error included in the systematics. A similar procedure was applied to the forward region where the efficiency was calculated to be $(66.3 \pm 2.2)\%$.

The only expected background was the small fraction of e^+e^- final state events (or τ events with high electromagnetic energy) missing both sets of VD hits and at least one TK (or both TPC track elements in the forward region). It was evaluated by using events generated with the BABAMC Monte Carlo program[10] and was found to be negligible.

The total systematic error was obtained by summing in quadrature the uncertainties in the trigger (Table 1) and selection efficiency corrections, the $\pm 0.5\%$ uncertainty in the luminosity measurement[11] and a $\pm 1\%$ error assumed on the radiative corrections. It is shown in Table 2 for the different energy points. In all cases the statistical error dominates.

Table 2 summarises the integrated luminosities, the number of selected events and the corresponding cross-sections (in the angular range $42^\circ < \theta < 138^\circ$) at each centre-of-mass energy. Table 3 summarises the number of events and the corresponding differential cross-section, corrected for the angular dependent detection and trigger efficiency, as a function

$\sqrt{s}$ (GeV)	Int. L (pb^{-1})	N$\gamma\gamma$	σ (pb)	σ_0 (pb)
91.25	36.87	503	$17.4 \pm 0.8 \pm 0.4$	18.3
130.4	2.86	23	$10.5 \pm 2.2 \pm 0.4$	8.97
136.3	2.96	19	$8.33 \pm 1.91 \pm 0.28$	8.21
161.5	9.58	44	$5.76 \pm 0.87 \pm 0.20$	5.85
172.4	9.80	35	$5.55 \pm 0.94 \pm 0.24$	5.13
182.7	52.99	179	$4.27 \pm 0.35 \pm 0.14$	4.57

Table 2: The integrated luminosities, the number of detected events (N$\gamma\gamma$), the measured cross-sections (σ) and the lowest order $e^+e^- \to \gamma\gamma$ QED predictions (σ_0) at different centre-of-mass energies. The first error is statistical, the second corresponds to the total systematic error. The cross-section of the previously published data [2] is given at the mean of the centre-of-mass energies weighted by the luminosity at each point. The cross-sections correspond to the angular range $42° < \theta < 138°$; the measured cross-sections have been corrected for radiative effects.

of $\cos\theta$. The experimental efficiency was obtained for the $\gamma\gamma(\gamma)$ events which passed the acceptance and acollinearity cuts at the generator level. The measured cross-sections reported in both tables were obtained after subtracting the radiative corrections [3] to the order α^3 so that they should correspond to the lowest order QED values. The lowest order QED values are included for comparison. The systematics on the cross sections of Table 3 are assumed to contribute as overall normalization errors of 3.4%, 3.4%, 4.4% and 3.3% for the four data sets.

4 Test of QED

The measured total and differential cross-sections after subtracting radiative corrections are shown in figures 3 and 4 respectively, together with the lowest order QED predictions. Only statistical errors are shown.

Possible deviations from QED are usually parametrised by adding to the QED differential cross-section a term depending on the cutoff parameters Λ_+ or Λ_- [13,14] :

$$\frac{d\sigma}{d\Omega} = \frac{\alpha^2}{s}\frac{1+cos^2\theta}{1-cos^2\theta}\left(1 \pm \frac{s^2}{2\Lambda_\pm^4}(1-cos^2\theta)\right) \qquad (1)$$

A maximum likelihood fit of expression (1) to the measured differential cross-sections at all the energies gave, for the parameter $\eta = 1/\Lambda^4$, a central value $\eta = (-1.4 \pm 1.5) \times 10^{-10}$ GeV^{-4}. This corresponds to lower limits at the 95% confidence level of $\Lambda_+ > 253$ GeV and $\Lambda_- > 225$ GeV. These are represented as the dashed and dotted lines in figure 4. The overall normalisation errors were taken into account in the fitting procedure and their contribution to the total error on η is $\pm 0.6 \times 10^{-10}$ GeV^{-4}. The published 1990-1992 DELPHI results [2] were also included in the fit. However, given the s^2 dependence of the non-QED term in eq.(1), the contribution of the Z^0 data was quite negligible; if these data are removed from the fit the limits are $\Lambda_+ > 250$ GeV and $\Lambda_- > 225$ GeV and if

[3] The radiative corrections are obtained as the difference between the cross-section of simulated $\gamma\gamma(\gamma)$ events [9] inside the acceptance and the lowest order QED prediction.

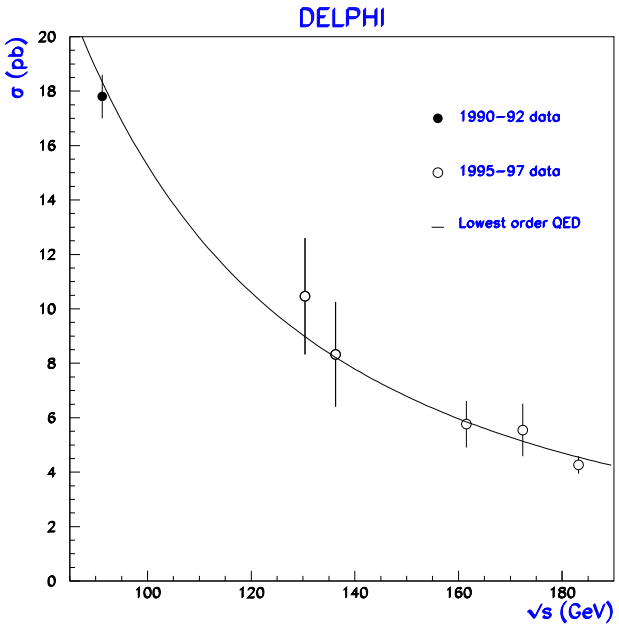

Figure 3: Total cross-section (in pb) for the process $e^+e^- \rightarrow \gamma\gamma(\gamma)$ in the region $42^\circ < \theta < 138^\circ$, as a function of the mean centre-of-mass energy for 1990-1992 data (black dot) , weighted by the luminosity at each point, and for the 1995-97 data (white dots). The solid line is the lowest order QED prediction.

the full statistical sample at the Z^0 would be included the expected improvement on the error on η is smaller than 3.5%.

For these and the following limits, the confidence level was obtained by normalising the probability to the integral over the region of definition of the parameters, as explained in Ref.[15]. The central values and their errors are quoted in order to allow them to be combined with the results of other experiments and to permit the evaluation of the confidence level by alternative methods[16]. The χ^2 of the data points with respect to the pure QED predictions is $\chi^2 = 27.3$ with 31 degrees of freedom.

5 Search for compositeness

The exchange of a virtual excited electron would modify the differential QED cross-section [13]. A likelihood fit was performed to the following expression, as a function of the excited electron mass (M_{e^*}) and the coupling constant (λ_γ):

$$\frac{d\sigma}{d\Omega} = \frac{\alpha^2}{s}\frac{1+cos^2\theta}{1-cos^2\theta}\left(1+\frac{s^2\lambda_\gamma^2}{2M_{e^*}^4}(1-cos^2\theta)H(cos^2\theta)\right) \qquad (2)$$

where $H(cos^2\theta) = a\frac{a+(1-cos^2\theta)/(1+cos^2\theta)}{(1+a)^2-cos^2\theta}$ and $a = 2M_{e^*}^2/s$. The fit was done over all data samples. Fig. 5 shows the resulting 95% confidence level limit on the (M_{e^*}, λ_γ/M_{e^*}) plane. In the mass region below 161 GeV/c^2 a better limit was obtained from the DELPHI search for t-channel production of e^*e [17]. For $\lambda_\gamma = 1$, the limit is $M_{e^*} > 231$ GeV/c^2 at the 95% confidence level, with a central value $1/M_{e^*}^4 = (-1.9 \pm 2.2) \times 10^{-10}$ (GeV/c^2)$^{-4}$.

6 Conclusions

The measured $e^+e^- \to \gamma\gamma(\gamma)$ cross-sections show good agreement with the QED predictions. Lower bounds were obtained on the QED cutoff parameters, $\Lambda_+ > 253$ GeV and $\Lambda_- > 225$ GeV as well as on the mass of an excited electron: $M_{e^*} > 231$ GeV/c^2 for $\lambda_\gamma = 1$. All the limits are at the 95% confidence level and are higher than the existing published results at lower energies [3].

Acknowledgements

We are greatly indebted to our technical collaborators, to the funding agencies for their support in building and operating the DELPHI detector, and to the members of the CERN-SL Division for the excellent performance of the LEP collider.
We are also grateful to the technical and engineering staffs in our laboratories and we acknowledge the support of:
Austrian Federal Ministry of Science, Research and Arts,
FNRS–FWO, Belgium,
FINEP, CNPq, CAPES, FUJB and FAPERJ, Brazil,
Czech Ministry of Industry and Trade, GA CR 202/96/0450 and GA AVCR A1010521,
Danish Natural Research Council,
Commission of the European Communities (DG XII),
Direction des Sciences de la Matière, CEA, France,
Bundesministerium für Bildung, Wissenschaft, Forschung und Technologie, Germany,
General Secretariat for Research and Technology, Greece,
National Science Foundation (NWO) and Foundation for Research on Matter (FOM), The Netherlands,
Norwegian Research Council,
State Committee for Scientific Research, Poland, 2P03B00108, 2P03B03311 and 628/E–78–SPUB–P03–023/97,
JNICT–Junta Nacional de Investigação Científica e Tecnológica, Portugal,
Vedecka grantova agentura MS SR, Slovakia, Nr. 95/5195/134,
Ministry of Science and Technology of the Republic of Slovenia,
CICYT, Spain, AEN96–1661 and AEN96-1681,
The Swedish Natural Science Research Council,
Particle Physics and Astronomy Research Council, UK,
Department of Energy, USA, DE–FG02–94ER40817.

References

[1] DELPHI Collab., P. Abreu et al., Phys. Lett. **B268** (1991) 296.
[2] DELPHI Collab., P. Abreu et al., Phys. Lett. **B327** (1994) 386.
[3] OPAL Collab., K Ackerstaff et al., Eur. Phys. J. **C1** (1998) 21 ;
ALEPH Collab., D. Buskulic et al., Phys. Lett. **B384** (1996) 333;
ALEPH Collab., R. Barate et al., CERN-EP/98-053 accepted by Phys. Lett.;
L3 Collab., M. Acciarri et al., CERN-PPE/97-77 submitted to Phys. Lett..
[4] DELPHI Collab., P. Abreu et al., Nucl. Inst. and Meth. **A303** (1991) 233.
[5] DELPHI Collab., P. Abreu et al., Nucl. Inst. and Meth. **A378** (1996) 57.
[6] DELPHI Collab., P. Aarnio et al., Nucl. Phys. B **367** (1991) 511.
[7] V. Chabaud et al., Nucl. Inst. and Meth. **A368** (1996) 314.
[8] P.Chochula et al., CERN-PPE 97-155, accepted by Nucl. Inst. and Meth..
[9] F.A. Berends and R. Kleiss, Nucl. Phys. B **186** (1981) 22.
[10] F.A. Berends, W. Hollik and R. Kleiss, Nucl. Phys. B **304** (1988) 712.
[11] D. Bardin et al., DELPHI note 93-101 (1993) unpublished;
S.J. Alvsvaaget al., DELPHI Collab., DELPHI note 95-68 (1995) Proceedings of EPS-HEP International Europhysics Conference Brussels 1995.
[12] B. Escoubes et al., Nucl. Inst. and Meth. **A257** (1987) 346.
[13] D. Treille et al., preprint ECFA 87-108 in: Compositeness at LEP II, CERN report 87-08 Vol. 2 (1987) p. 414.
[14] S. Drell, Ann. Phys. (NY) **4** (1958) 75;
F.E. Low, Phys. Rev. Lett. **14** (1965) 238.
[15] Particle Data Group, R. M. Barnett et al., Phys. Rev. D **54** part 1 (1996) 164.
[16] F. James and M. Roos, Phys. Rev. D **44** (1991) 299.
[17] DELPHI Collab., P. Abreu et al., Phys. Lett. **B393** (1997) 245.

$cos\theta$	$d\sigma_0/d\Omega$ (pb/sr)	$d\sigma/d\Omega$ (pb/sr)	Number of events
133 GeV			
0.035-0.136	1.18	$2.05^{+0.97}_{-0.74}$	6
0.136-0.237	1.25	$1.57^{+0.83}_{-0.61}$	5
0.237-0.338	1.38	$0.91^{+0.65}_{-0.44}$	3
0.338-0.440	1.58	$1.26^{+0.75}_{-0.54}$	4
0.440-0.541	1.90	$1.79^{+0.85}_{-0.64}$	6
0.541-0.642	2.42	$1.85^{+0.88}_{-0.67}$	6
0.642-0.743	3.31	$3.88^{+1.30}_{-1.06}$	11
161 GeV			
0.035-0.136	0.81	$0.21^{+0.32}_{-0.16}$	1
0.136-0.237	0.85	$0.80^{+0.48}_{-0.34}$	4
0.237-0.338	0.94	$1.73^{+0.65}_{-0.52}$	9
0.338-0.440	1.08	$0.99^{+0.52}_{-0.38}$	5
0.440-0.541	1.30	$1.69^{+0.64}_{-0.51}$	9
0.541-0.642	1.65	$1.16^{+0.55}_{-0.42}$	6
0.642-0.743	2.26	$2.23^{+0.79}_{-0.64}$	10
0.844-0.906	6.00	$8.93^{+2.22}_{-1.90}$	19
172 GeV			
0.035-0.136	0.71	$0.52^{+0.48}_{-0.29}$	2
0.136-0.237	0.75	$1.20^{+0.63}_{-0.47}$	5
0.237-0.338	0.82	$0.93^{+0.56}_{-0.40}$	4
0.338-0.440	0.95	$0.47^{+0.44}_{-0.27}$	2
0.440-0.541	1.14	$1.36^{+0.65}_{-0.49}$	6
0.541-0.642	1.45	$1.63^{+0.70}_{-0.55}$	7
0.642-0.743	1.98	$2.42^{+0.91}_{-0.73}$	9
0.844-0.906	5.27	$5.05^{+1.70}_{-1.38}$	11
183 GeV			
0.035-0.136	0.63	$0.49^{+0.15}_{-0.13}$	13
0.136-0.237	0.67	$0.84^{+0.19}_{-0.16}$	23
0.237-0.338	0.73	$0.60^{+0.15}_{-0.13}$	18
0.338-0.440	0.84	$0.50^{+0.16}_{-0.13}$	12
0.440-0.541	1.01	$0.76^{+0.17}_{-0.15}$	23
0.541-0.642	1.29	$1.25^{+0.22}_{-0.20}$	35
0.642-0.743	1.77	$2.05^{+0.29}_{-0.27}$	53
0.844-0.906	4.69	$5.14^{+0.70}_{-0.64}$	59

Table 3: The lowest order $e^+e^- \to \gamma\gamma$ QED predictions ($d\sigma_0/d\Omega$), the measured differential cross-sections ($d\sigma/d\Omega$) and the number of detected events for different $\cos\theta$ regions. The quoted errors are statistical only computed following the Bayesian approach (minimal interval) for small number of events [12]. The measured cross-sections were corrected for radiative effects. The systematics is assumed to contribute as an overall normalization error being 3.4%, 3.4%, 4.4% and3.3% for the four data sets, respectively

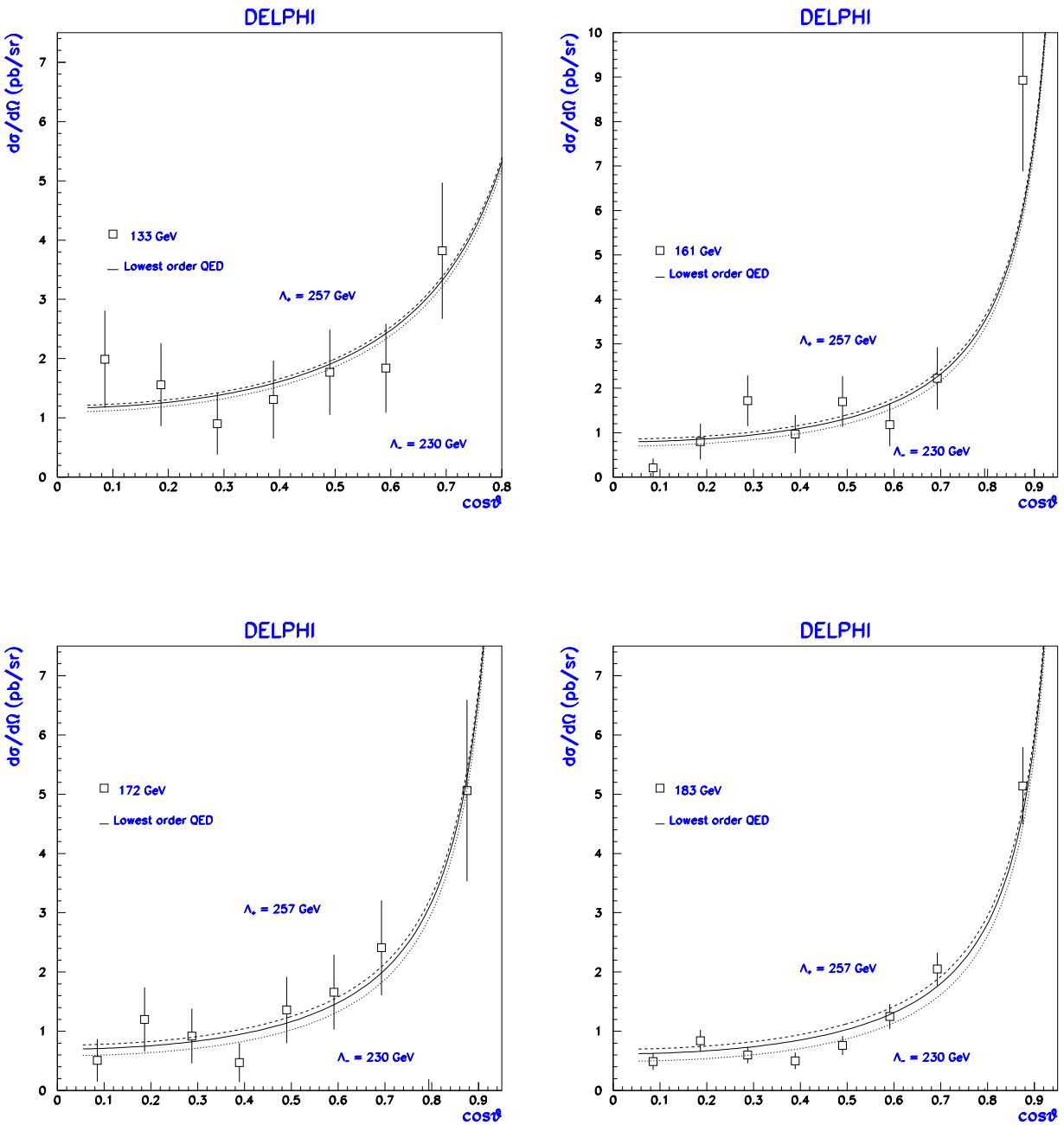

Figure 4: Differential cross-section, $d\sigma/d\Omega$, for the process $e^+e^- \to \gamma\gamma(\gamma)$ at the centre-of-mass energies of 133.3 GeV (mean of the 1995 130.4 GeV and 136.3 GeV points), 161.5 GeV, 172.4 and 182.7 GeV. The solid curves show the lowest order QED prediction. The dashed (dotted) curves show the derived limit on the prediction parametrised by Λ_+ (Λ_-).

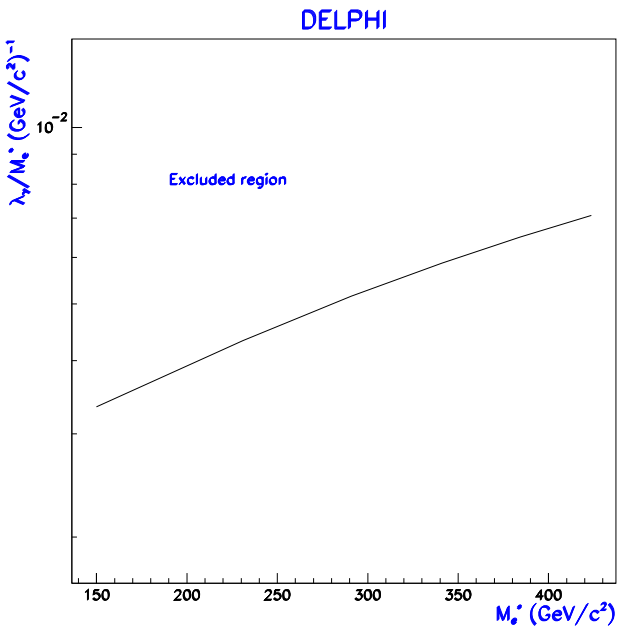

Figure 5: Upper limit on the effective coupling constant λ_γ/M_{e^*} versus M_{e^*}. For $M_{e^*} < 161$ GeV/c^2 a better limit was obtained by a direct search[17].